Investigation on the Use of a Passive Nonlinear Absorber for the Reduction of Vibration in the Mast of a Floating Offshore Wind Turbine

Antonio Cillis, Emmanuelle Sarrouy, Pierre-Olivier Mattei, Riccardo Mariani, Thomas Choisnet

MADRID
inter.noise 2019
June 16 - 19
NOISE CONTROL FOR A BETTER ENVIRONMENT

Investigation on the Use of a Passive Nonlinear Absorber for the Reduction of Vibration in the Mast of a Floating Offshore Wind Turbine

Antonio Cillis[1]
Ecole Centrale de Lyon
36 Avenue Guy de Collongue, 69134 Écully, France

Emmanuelle Sarrouy[2]
Aix Marseille Univ, CNRS, Centrale Marseille, LMA
4 Impasse Nikola Tesla, 13013 Marseille, France

Pierre-Olivier Mattei[3]
Aix Marseille Univ, CNRS, Centrale Marseille, LMA
4 Impasse Nikola Tesla, 13013 Marseille, France

Riccardo Mariani[4]
Ideol
375 avenue du Mistral, 13600 La-Ciotat, France

Thomas Choisnet[5]
Ideol
375 avenue du Mistral, 13600 La-Ciotat, France

ABSTRACT

Floating Offshore Wind Turbines (FOWT's) are subjected to different types of dynamic loads such as environmental loads (wave and wind), aero-structure interaction loads and mechanical loads (inertial and controller effects). These loads induce vibrations in the WT mast that are transmitted in the floating foundation and mooring lines, increasing the overall ultimate loads and fatigue cycling.

In this paper the potentiality of a passive nonlinear mechanical system for the reduction of WT mast vibrations is studied. This kind of absorber called Nonlinear Energy Sink (NES) is based on the energy pumping phenomenon.

The feasibility and efficiency of the absorber is first demonstrated by means of a simplified full-scale numerical model composed of two degrees of freedom, one for the WT mast (first bending mode) and one for NES.

Then, an equivalent reduced scale model is considered and analyzed by numerical simulations and experiments.

[1] antonio.cillis@auditeur.ec-lyon.fr
[2] emmanuelle.sarrouy@centrale-marseille.fr
[3] mattei@lma.cnrs-mrs.fr
[4] riccardo.mariani@ideol-offshore.com
[5] thomas.choisnet@ideol-offshore.com

The study is concluded with the sizing of an optimized absorber for the full-scale system. Some sensitivity analyses considering variations of the mast structural characteristics (stiffness and structural damping) are performed to investigate the NES efficiency limits, confirming the performances of the NES: reduction of vibratory level around 8-10 dB over a large range of functioning loads.

Keywords: …

I-INCE Classification of Subject Number: 54
http://i-ince.org/files/data/classification.pdf

Table des matières

1. INTRODUCTION

…

(All)

2. BACKGROUND

2.1. Dynamics of floating offshore wind turbine

Modal behavior of wind turbines: results of FEM modal analysis performed on DTU10MW (in onshore configuration) and discussion.
Impact of boundary condition and added mass (WT fixed on floating structure) on first modes.

(Riccardo)

Description of sources of dynamic excitation of floating wind turbines:

- interaction rotor-mast generating load at frequencies 1P, 3P, …
- environmental loads (waves and wind)

and impact on the design of FWT's.
Presentation of Cambell diagram of a FWT, different design philosophies for the mast of a generic WT (stiff-stiff, soft-stiff and soft-soft) and discussion on the best choice for floating offshore application (stiff-stiff)

(Thomas)

2.2. Energy pumping and NES

Description of theory of energy pumping and NES and their main applications.
[…] Conclude this general overview with the current NES technology:
(Emmanuelle et Pierre-Olivier)

Here, a bistable NES based on a buckled plate with length l_N, height h_N and thickness e_N will be used. This plate supports a concentrated mass M_P at its mid-length. The whole apparatus is maintained and attached to the structure by a rigid support with mass M_S as depicted in Figure 1.

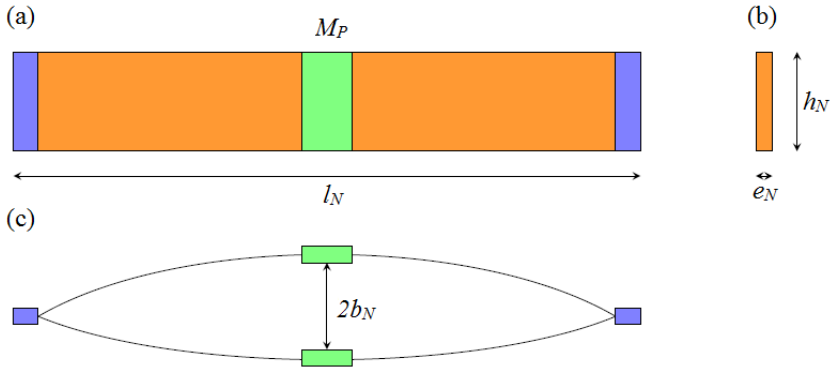

Figure 1. Bistable NES sketch. (a) Lateral view (b) Plate cross-section dimensions (c) Top view of buckled plate stable positions.

3. MODELLING AND SIMULATIONS

In order to have fast computations, simplified models are used for simulations. Hence, the next sections present first the studied wind turbine and some of its dynamics characteristic; then, the reduced wind turbine model and the associated NES model equations are provided before showing results for a full scale model and a reduced (experimental) model.

3.1. Wind turbine

Description of the wind turbine DTU10MW: main characteristics, rotation speed, thrust and power curves.
Results of preliminary simulations in FAST for the characterization of dynamic loads (in particular harmonic excitation at 3P frequency)

(Riccardo)

3.2. Wind turbine with NES model

Excitation sources have very low frequencies compared to the turbine modes higher than 1. Hence, a simple model for whole WT is built considering only 1 dof (degree of freedom). To this end, the turbine geometry is first simplified: the mast is represented as a beam with length h_p and square section (inside and outside lengths denoted b_1 and b_2 respectively) and the turbine at its top end is reduced to a concentrated mass M_T undergoing a harmonic force $F(t)=A\cos(\omega t)$ as depicted in Figure 2.

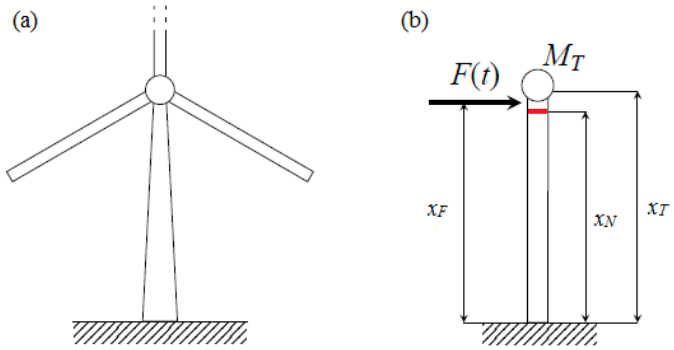

Figure 2 Reduced turbine model. (a) Original geometry; (b) Simplified model including the NES (red line).

The lateral deflection $w(x,t)$ along the beam is then governed by the following equation (assuming an Euler-Bernoulli model):

$$(1) \quad EI\frac{\partial^4 w}{\partial x^4} + \left(\rho S + M_T\delta_{x_T}(x) + M_N\delta_{x_N}(x)\right)\frac{\partial^2 w}{\partial t^2} = \delta_{x_F}(x)A\cos(\omega t) \quad (t)$$

where E is the beam material Young modulus, ρ is its density, $S=b_2^2-b_1^2$ the beam cross-section area and $I=(b_2^4-b_1^4)/12$ its second moment of area, M_N is the total mass of the NES apparatus and δ_x denotes the Dirac distribution at point x. Beam section dimensions b_1 and b_2 were chosen so that the total mass is equal to total mast mass and that the second moment of area of the beam is equal to the one of the mast at middle height $h_p/2$.

The second step to obtain the final beam model is to reduce the displacement field w to be proportional to the first eigenshape of the beam alone, $\phi(x)$: $w(x,t) = \phi(x)u(t)$. When introducing damping μ_B, Equation (1) becomes:

(2) $m_B\,\ddot{u}+\mu_B\,\dot{u}+k_B u = \phi(x_F)A\cos(\omega t)$

with $m_B=\rho S+M_T\,\phi^2(x_T)+M_N\,\phi^2(x_N)$ the dynamic mass and $k_B = \int_0^{h_T} EI\frac{\partial^4\phi}{\partial x^4}\phi\,dx$ the dynamic stiffness.

After a few transformations and assumptions [2], the bistable NES behavior can be described as follows:

(3) $m_N\,\ddot{q} + \mu_N\,\dot{q} + k_N F_{nl}(q) = 0$

where m_N, μ_N and $k_N=(2\pi\,f_N)^2$ are the dynamic mass, damping and stiffness respectively. $m_N = (3/8)\,\rho_N S_N l_N + M_p$; μ_N and k_N are identified experimentally.

Coupling both structures gives:

(4) $$\begin{cases} m_B\,\ddot{u}+\mu_B\,\dot{u}+k_B u - \mu_N(\dot{q}-\phi(x_N)\dot{u}) - k_N F_{nl}(q-\phi(x_N)u) = \phi(x_F)A\cos(\omega t) \\ m_N\,\ddot{q} + \mu_N(\,\dot{q}-\phi(x_N)\dot{u}) + k_N F_{nl}(q-\phi(x_N)u) = 0 \end{cases}$$

3.3. Full scale model simulations

Model described in Equation (4) is simulated using a Mathematica code for various excitation frequencies ω and amplitudes A when considering the full scale model.

NES dimensions were chosen based on the NES studied in [2] with a ×70 scale factor. They were then manually adjusted to find a first satisfying results set. Numerical values used for these simulations are given in Table 1. An optimization process will be applied later to the NES parameters in Sec. 5.1.

Lengths and Turbine mass			
$L=x_T$ = 94.3 m	x_F = 93.5 m	x_N = 93.5 m	M_T = 675000 kg
Beam properties			
E = 210 GPa	ρ = 7800 kg.m^{-3}	b_1 = 7.448 m	b_2 = 7.529 m
$\mu_B = 2\times0.05(2\pi f_B)$			
NES properties			
l_N = 7 m	b_N = 0.35 m	h_N = 0.35 m	e_N = 7 10^{-3} m
E_N = 200 GPa	ρ_N = 7800 kg.m^{-3}	f_N = 0.55 Hz	$\mu_N = 2\times0.025(2\pi f_N)$
M_P = 1 300 kg	M_S = 14 000 kg		

Table 1. Numerical values for full scale model.

These values give a first eigenfrequency f_B = 0.477 Hz for the beam plus turbine mass alone which is very close to the real problem first eigenfrequency (0.48 Hz). NES first eigenfrequency is taken equal to 0.55 Hz that is higher than the structure one with a relatively small damping rate (2.5 %). The frequency response function (FRF) is displayed in Figure 3(a): as expected the NES becomes active when excitation amplitude is large enough and "cuts" the structure response amplitude for a wide range of frequencies. Figure 3(b) displays the ridge curves for simulations with and without the NES being active (its added mass is always considered): for each excitation amplitude, the maximum value of the structure response amplitude over the whole frequency range is displayed. As expected, the ratio structure response over excitation amplitudes is constant when the NES is inactive, hence, the model is linear. When the

NES is active however, a reduction up to 9 dB is obtained which is very encouraging and justifies the rest of the study.

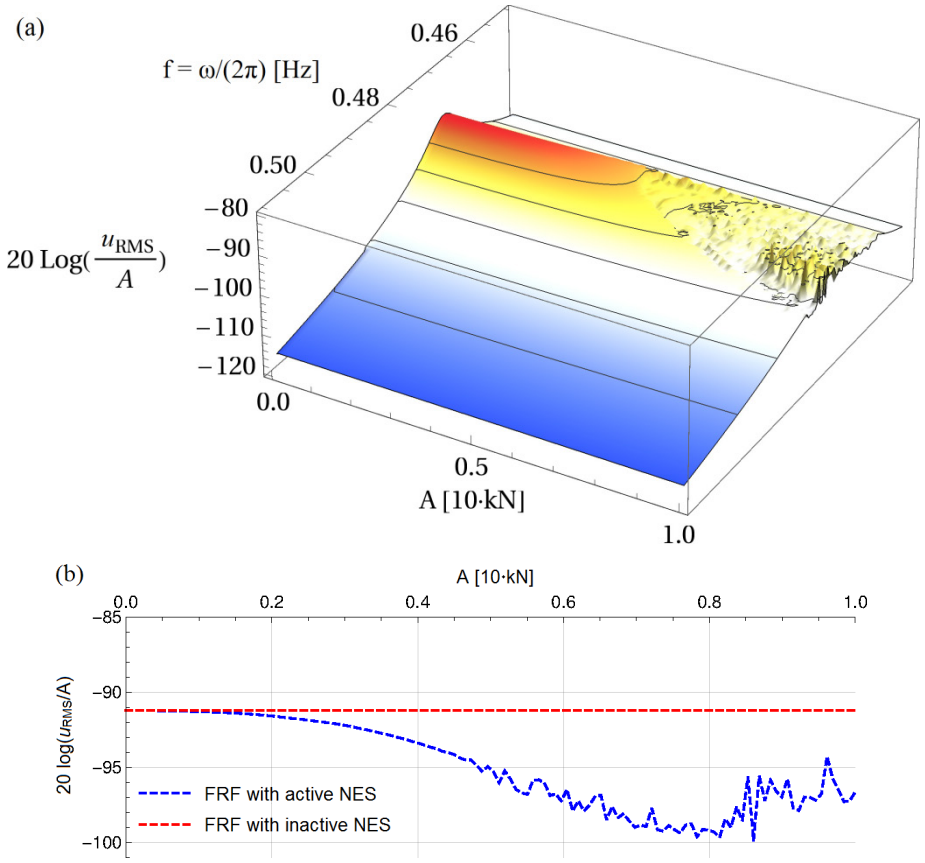

Figure 3.Full scale model results: (a) FRF (b) ridge curves with and without NES.

3.4. 1:100 scale model simulations

The next step will be to validate numerical results using an experimental set-up. As a full scale experimental campaign would be very costly to realize, a 1:100 scale model is first numerically designed before being experimentally tested.

Using a dimensionless abscissa $s=x/L$ and displacement $v(s,t)=w(sL,t)/L$, Equation (1) becomes, when divided by ρS and putting the NES added mass aside:

$$(5) \quad \frac{EI}{\rho S L^4}\frac{\partial^4 v}{\partial s^4} + \left(1 + \frac{M_T}{\rho S L}\delta_{s_T}(s)\right)\frac{\partial^2 v}{\partial t^2} = \delta_{s_F}(s)\frac{A}{\rho S L}\cos(\omega t) \quad (t)$$

Now, to build a reduced model with ρ', E', I', L', S', M_T', M_N' and A' characteristics with preserves added mass ratio, first eigenfrequency and external loading one has to satisfy the following three equations:

$$(6) \quad \frac{M_T}{\rho S L} = \frac{M_T'}{\rho' S' L'} \quad , \quad \frac{EI}{\rho S L^4} = \frac{E'I'}{\rho' S' L'^4} \quad \text{and} \quad \frac{A}{\rho S L} = \frac{A'}{\rho' S' L'}$$

As the beam material is steel for both full scale and reduced scale models ($E=E'$, $\rho=\rho'$), one gets the properties for the equivalent beam with plain rectangular section (length L', width h' and thickness e' displayed in Table 2.

NES properties are chosen by starting from values described in [2] and modifying them until a satisfying result is obtained.

Lengths and Turbine mass			
$L'=x_T'$ = 1.28 m	x_F' = 1.26 m	x_N' = 1.20 m	M_T' = 0.8 kg
Beam properties			
E' = 210 GPa	ρ' = 7800 kg.m^{-3}	h' = 5 10^{-2} m	e' = 2 10^{-3} m
μ_B' = 2×0.05$(2\pi f_B)$			
NES properties			
l_N' = 0.102 m	b_N' = 0.6 10^{-3} m	h_N' = 0.01 m	e_N' = 0.2 10^{-3} m
E_N' = 200 GPa	ρ_N' = 7800 kg.m^{-3}	f_N' = 0.54 Hz	μ_N'=2×0.026$(2\pi f_N)$
M_P' = 12 10^{-3} kg	M_S = 30 10^{-3} kg		

Table 2. Numerical values for reduced (1:100) scale model.

Results obtained for this reduced scale model with values in Table 2 are presented in Figure 4.This configuration provides a beam vibration amplitude reduction up to 11 dB.

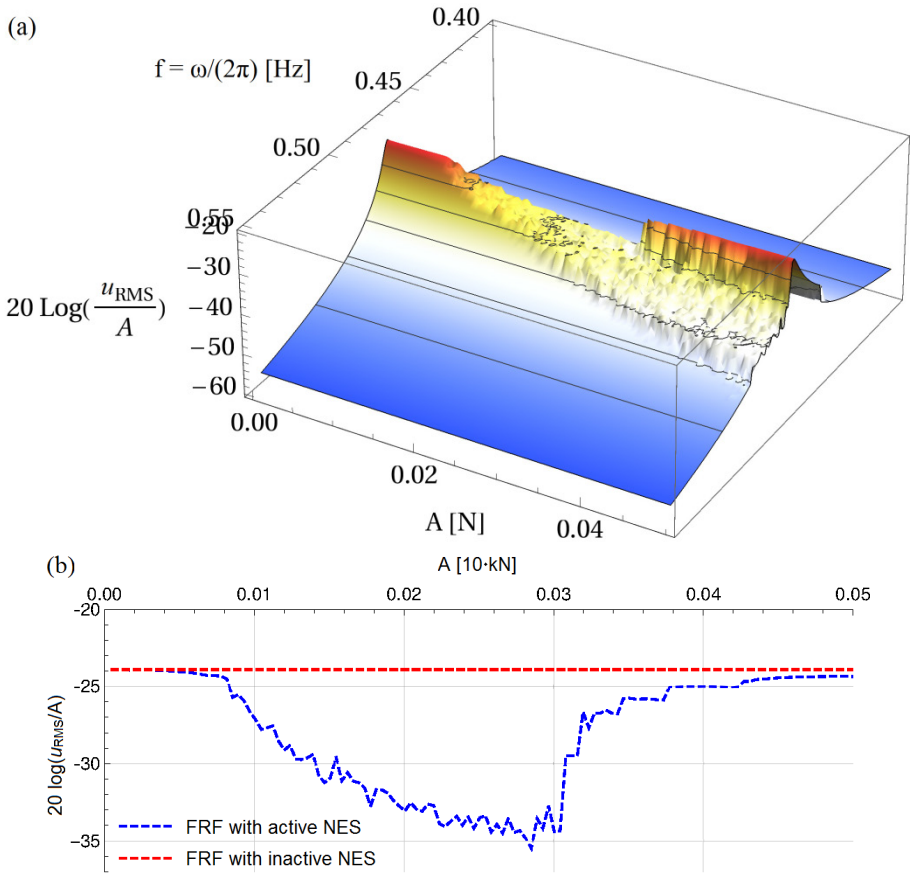

Figure 4.Reduced scale model results: (a) FRF (b) ridge curves with and without NES.

4. EXPERIMENTAL VALIDATION

The objective of this section is to validate the promising results obtained numerically using an experimental set-up.

4.1. Experimental set-up and test program

A beam with plain rectangular section close to the one designed and tested in Sec. 3.4 is used. Its real parameters are provided in Table 3 along with NES and other parameters. It is to be noted that, for instrumentation purpose, the beam is horizontal rather than vertical.

Lengths and Turbine mass				
L^e = 1,3 m	x_T^e = 0.945 m	x_F^e = 1.26 m	x_N^e = 1.28 m	M_T^e = 0.802 kg
Beam properties				
E^e = 210 GPa	ρ^e = 7800 kg.m^{-3}	h^e = 3 10^{-2} m	e^e = 4 10^{-3} m	
μ_B^e=2×0.008$(2\pi f_B)$	f_B^e = 1.1353 Hz			
NES properties				
l_N^e = 0.12 m	b_N^e = 2 10^{-3} m	h_N^e = 0.05 m	e_N^e = 0.5 10^{-3} m	
E_N' = 200 GPa	ρ_N' = 7800 kg.m^{-3}	f_N^e = 4.25 Hz	μ_N^e=2×0.02$(2\pi f_N^e)$	
M_P' = 23 10^{-3} kg	M_S = 80 10^{-3} kg			
Sensors locations				
x_{uF} = 0.078 m	x_{uB} = 0.512 m	x_{vB} = 0.945 m	x_{uN} = 1.352 m	

Table 3. Numerical values for experimental set-up

Figure 5 shows a photo as well as a sketch of the experimental set-up. An excitation is applied at the bottom of the beam using a type 4810 Brüel & Kjær shaker associated to a type 2706 Brüel & Kjær amplifier. Three laser displacements sensors (Keyence LK-G32, LK-G82 and LKG-152) monitor the excitation induced displacement u_F, an intermediate beam displacement u_B and the NES displacement u_N respectively. Finally, a Polytec PSV-400 laser vibrometer driven by an OFV-400 controller measures the beam velocity v_B closer to the mass.

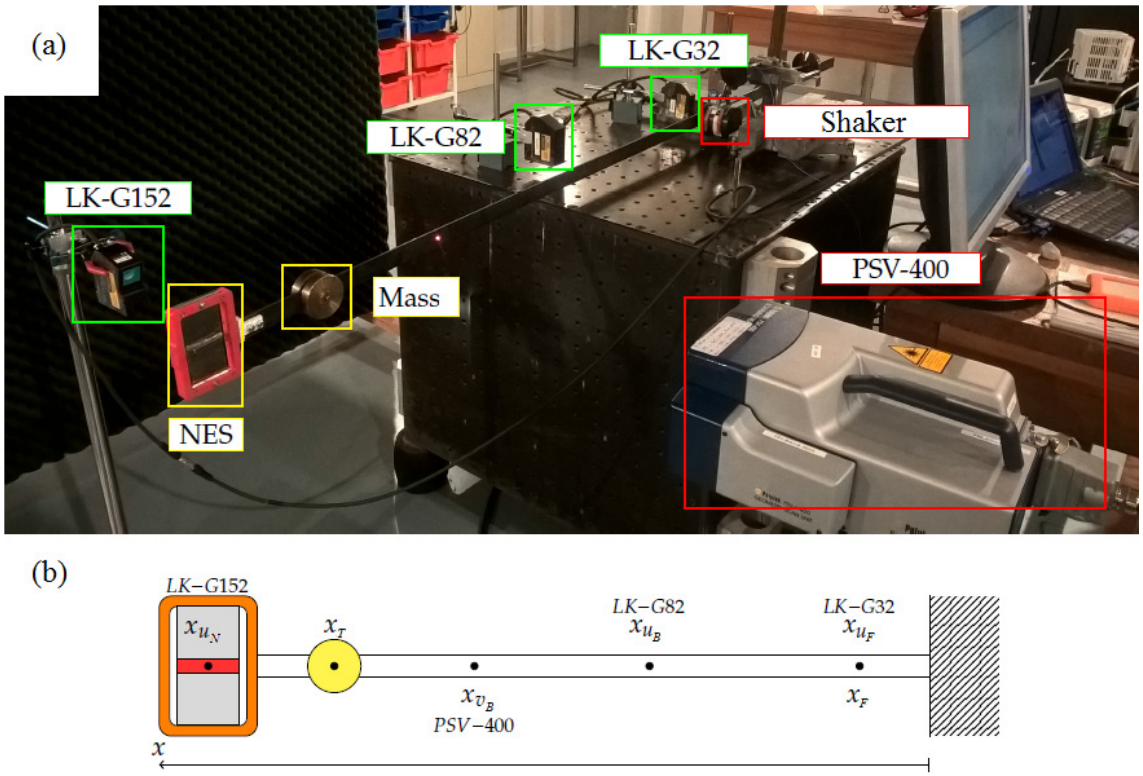

Figure 5. Experimental set-up: (a) photo; (b) sketch with important abscissa.

A first series of tests are run with white noise excitation with small amplitudes A so as to stay in the linear regime. First, the configuration is as depicted in Figure 5 and the excitation amplifier is set to A = 0.1 V. This provides the beam dynamical properties f_B^e = 1.13 Hz and μ_B^e (as well as higher modes) but the NES first mode does not appear as

can be seen on Figure 6(a). Then the beam is excited but without the turbine mass M_T and still very small excitation amplitudes (A = 0.025 V). Removing the mass M_T makes the beam eigenfrequencies higher and let the NES first mode appear (cf. Figure 6(b)). Hence, its dynamical properties f_N^e = 4.25 Hz and μ_N^e can be identified.

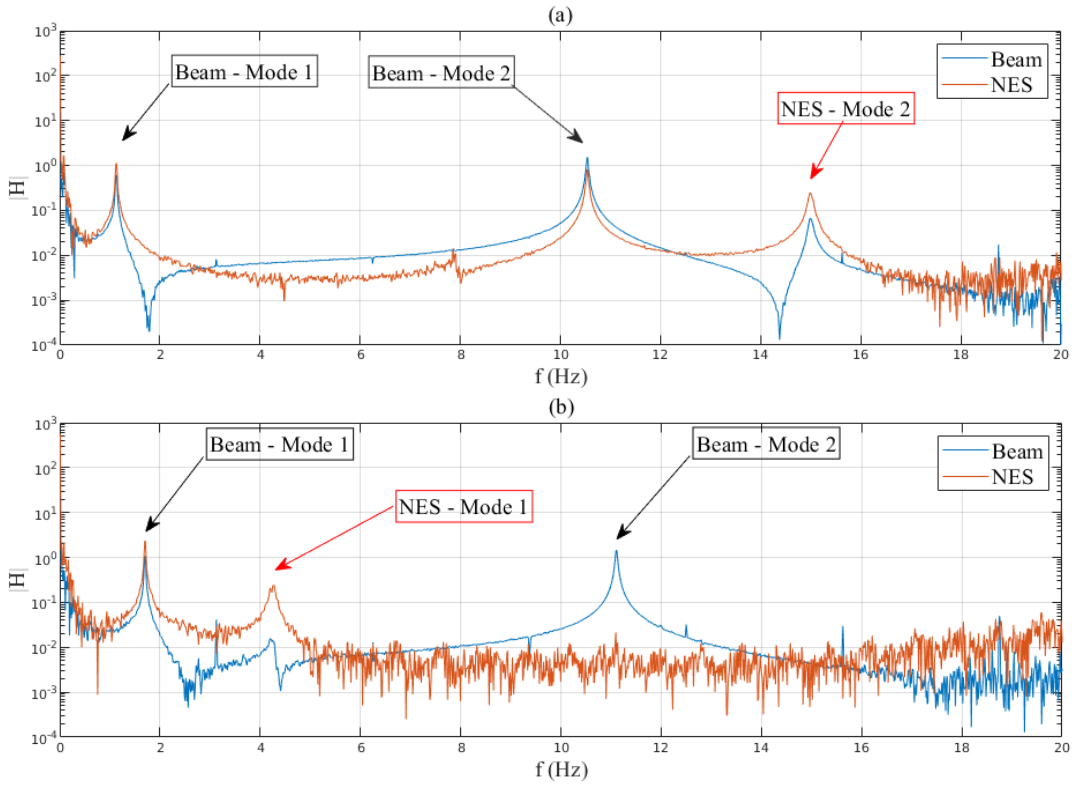

Figure 6. Experimental FRF for (a) complete structure and (b) structure without M_T.

These first measures indicate that the NES first frequency is higher than expected (about 3 times the beam first mode).

4.2. Results of the tests with white noise excitation

Results of white noise tests varying excitation level for configuration 2: observation of vibration reduction (pumping) on the 2nd mode of the beam.

4.3. Results of the tests with sinusoidal excitation

Results of sinusoidal excitation tests on configuration 1 and 2 for different levels of excitation, tuning of numerical model (determination of tension/applied force ratio) and comparison experimental/numerical results.

(Emmanuelle et Pierre-Olivier)

5. OPTIMIZATION OF THE NES AND SENSITIVITY STUDY

5.1. Optimal sizing of NES

Numerical results of pumping with optimized NES.

5.2. Sensitivity analysis on structural parameters of the WT mast

Numerical results for different stiffness and different structural damping of the mast. (Emmanuelle et Pierre-Olivier)

6. CONCLUSIONS

(All)

7. ACKNOWLEDGEMENTS

?

8. REFERENCES

1. Hau, E., "*Wind Turbines – Fundamentals, Technologies, Application, Economics – 2nd edition*", Springer-Verlag, Berlin Heidelberg (2006)
2. P.-O. Mattei, R. Ponçot, M. Pachebat, R. Côte, *Non-linear targeted energy transfer of two coupled cantilever beams coupled to a bistable light attachment*, Journal of Sound and Vibration, vol. 337, pp. 29-51 (2016)

1. INTRODUCTION

The INTER-NOISE 2019 MADRID Proceedings will be distributed to the congress participants on a memory stick.

The purpose of these instructions is to ensure the uniformity of the publication.

The manuscript should be submitted as **MS-Word PDF file, 12-point "Times New Roman",** if available. The maximum length of the manuscript should not be more than **12 pages**, except for plenary lectures, and with a minimum of four pages

Only manuscripts in English will be accepted for inclusion in the Proceedings.

Please, do not insert any page numbers and do not include any headers of foot notes, except in the first page of the manuscript for the e-mail addresses.

[1] aaa.bbb@madrid.es
[2] bbb@ spain.com

2. MANUSCRIPT FORMAT

2.1 Margin Settings

- Paper size A4
- Margin settings: Top: 2.5 cm; Bottom: 2.5 cm; Left: 3.0 cm; Right: 3.0 cm
- Text justified left and right
- Indent first line of the paragraphs by 0.5 cm

2.2 Paragraphs

- Leave one line between headings and subheadings
- Major headings shall be numerically ordered as **1.** , **2.** , etc., bold type
- Level 2 subheading **2.1** , **2.2** , etc., bold type

2.3 Figures, Tables and Equations

All figures, tables, equations, photos, graphs, etc., must be included shortly after the mention, centered in the page.

The caption of figures and photos below in italics.

The equations should be referenced as Equation 1, Equation 2, etc.

The caption of tables placed just above in italics and numbered Table 1.Table 2, etc..

3. IMPORTANT INFORMATION

3.1 Submission of Manuscripts

Submit your manuscript as a PDF file using the link on the INTER-NOISE 2019 website (www.internoise2019.org).

Before submitting the manuscript you will be required to pay at least one registration. Additionally, if you are submitting more than one manuscript, there is an additional nominal charge for each additional manuscript submitted.

3.2 Conversion to PDF

Carefully inspect your PDF file before submission to be sure that the PDF conversion was done properly and that there are no errors when you open the PDF file. Common problems are: missing or incorrectly converted symbols especially

mathematical symbols, failure of figures to reproduce, and incomplete legends in figures. Identification and correction of these problems is the responsibility of the authors. Your manuscript will publish in the Congress Proceeding as it is received.

4. CONCLUSIONS

Please follow these manuscripts preparation instructions carefully.

5. ACKNOWLEDGEMENTS

We acknowledge gratefully the authors for submitting their work to INTER-NOISE 2019 MADRID.

6. REFERENCES

1. Leo L. Beranek and István L. Vér, *"Noise and Vibration Control Engineering – Principles and Applications"*, edited by Leo L. Beranek and István L. Vér, John Wiley & Sons, New York (2006)

2. L. Cremer, M. Heckl, B.A.T. Petersson, *"Structure-Borne Sound - Structural Vibrations and Sound Radiation at Audio Frequencies",* Springer (2005)